RESEARCH ARTICLE

small methods
www.small-methods.com

Nanopore Identification of L-, D-Lactic Acids, D-Glucose and Gluconic Acid in the Serum of Human and Animals

*Wendong Jia, Yusheng Ouyang, Shanyu Zhang, Panke Zhang, and Shuo Huang**

DL-Lactic acid and D-glucose are important human health indicators. Their aberrant levels in body fluids may indicate a variety of human pathological conditions, suggesting an urgent need of daily monitoring. However, simultaneous and rapid analysis of DL-lactic acid and D-glucose using a sole but simple sensing system has never been reported. Here, an engineered *Mycobacterium smegmatis* porin A (MspA) nanopore is used to simultaneously identify DL-lactic acid and D-glucose. Highly distinguishable nanopore event features are reported. Assisted with a custom machine learning algorithm, direct identification of DL-lactic acid and D-glucose is performed with human serum, demonstrating its sensing reliability against complex and heterogeneous samples. This sensing strategy is further applied in the analysis of different animal serum samples, according to which gluconic acid is further identified. The serum samples from different animals report distinguishable levels of DL-lactic acid, D-glucose and gluconic acid, suggesting its potential applications in agricultural science and breeding industry. This sensing strategy is generally direct, rapid, economic and requires only ≈µL of input serum, suitable for point of care testing (POCT) applications.

1. Introduction

L-Lactic acid is the final metabolite of glycolysis in many organisms under anaerobic conditions.[1] D-Lactic acid, the chiral isomer of L-lactic acid, is however produced by bacteria in gastrointestinal tract or is converted by other microorganisms in vivo.[2] Thus, when the gastrointestinal tract and intestinal barrier function are impaired, large amounts of D-lactic is accumulated in the body.[2] Generally, a variety of physiological and pathological conditions are associated with lactic acid. Excessive lactic acid in serum may also lead to hyperlactatemia and lactic acidosis.[3] Serum lactate is also used as a fitness indicator.[4] Monitoring of lactic acid is also widely used in the quality control of dairy products and wine fermentation.[5]

D-glucose is the metabolic substrate and the energy supplier of almost all living organisms.[6] The glucose level in living organisms is associated with many pathologic conditions, including cancer, diabetes and obesity.[7,8] Thus, simultaneous analysis of lactic acid and glucose in serum is important for disease diagnosis and personal health monitoring. Particularly, for the diagnosis of lactic acidosis caused by some acute complications of diabetes, simultaneous detection of lactic acid and glucose levels are necessary.[9,10] Gluconic acid, an oxidation product of glucose, is beneficial to maintain the activities of various digestive enzymes by regulating the pH of gastrointestinal tract. It is usually used as a feed additive or produced due to the addition of glucose oxidase to the fodder in breeding industry.[11,12]

Conventional methods, which rely on corresponding enzymatic reactions, have been widely used for the determination of L-lactic acid[13,14] and D-glucose[15,16] in body fluids. The assay based on lactate oxidase (LOX), which essentially detects H_2O_2 produced by the corresponding oxidase, has a similar principle of D-glucose sensing by the glucose oxidase. Thus, simultaneous sensing of D-glucose and L-lactic acid by the oxidase strategy may be conflicting. By developing D-lactate dehydrogenase (D-LDH), which has an enzyme activity against the D-lactic acid, sensing of D-lactic acid could be performed.[17,18] However, some endogenous compounds such as L-lactic acid and pyruvate, may still interfere with the reaction of D-LDH.[19] Some non-enzymatic methods, such as liquid chromatography-tandem mass spectrometry (LC-MS/MS)[20,21] and aptamers,[22] are also used in the detection of DL-lactic acid and D-glucose. However, the discrimination between DL-lactic acid still requires additional chiral chromatography operations.[21] The facility of LC-MS/MS is also bulky and requires special expertise for the operation. The aptamers are deficient in the detection resolution and the sensitivity, and requires additional reporting methods, such as fluorophores.[22] Thus, the development of a miniaturized, rapid and economic method for simultaneous identification of L-, D-lactic acid and D-glucose in serum, which is advantageous for corresponding medical diagnosis or daily monitoring of personal health conditions, may require a different sensing principle.

W. Jia, Y. Ouyang, S. Zhang, P. Zhang, S. Huang
State Key Laboratory of Analytical Chemistry for Life Sciences
School of Chemistry and Chemical Engineering
Nanjing University
Nanjing 210023, China
E-mail: shuo.huang@nju.edu.cn
W. Jia, Y. Ouyang, S. Zhang, S. Huang
Chemistry and Biomedicine Innovation Center (ChemBIC)
Nanjing University
Nanjing 210023, China

The ORCID identification number(s) for the author(s) of this article can be found under https://doi.org/10.1002/smtd.202400664

DOI: 10.1002/smtd.202400664

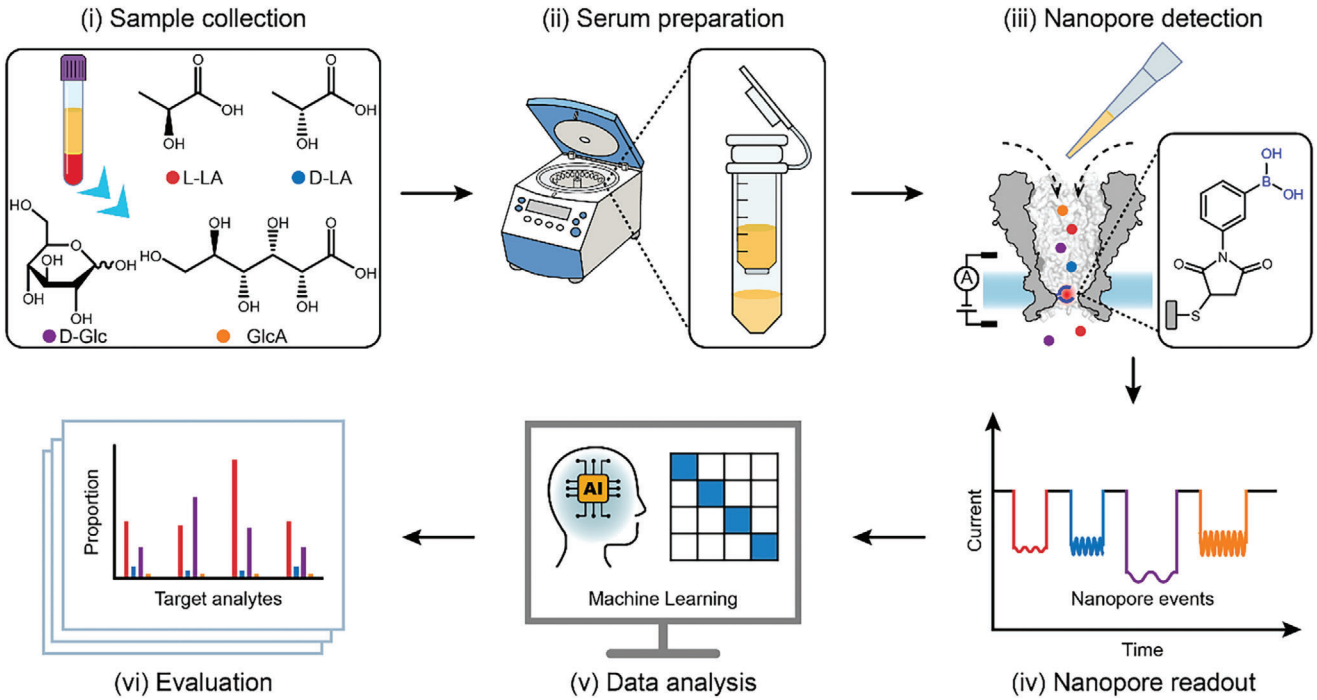

Scheme 1. The workflow of nanopore serum analysis. i) Blood serum is acquired by centrifugation after coagulation. L-lactic acid (L-LA), D-lactic acid (D-LA), D-glucose (D-Glc) and gluconic acid (GlcA) are targets of analysis. ii) The ultrafiltrate of the serum is then collected. iii) The filtrate is further added to the nanopore sensing device. A functionalized *Mycobacterium smegmatis* porin A (MspA) nanopore containing a sole phenylboronic acid (PBA) adapter, is used for molecular identification. L-lactic acid, D-lactic acid, D-glucose and gluconic acid all contain *cis*-diols moiety, enabling their reversible interaction with the PBA adapter of MspA-90PBA to report corresponding nanopore events. iv) The L-, D-lactic acid, D-glucose and gluconic acid can reversibly bind to and dissociate from the PBA adapter, generating characteristic event features for molecular identification. v) A custom machine learning algorithm serves to automatically identify target and interfering events. vi) The classified results are further investigated for serum.

Biological nanopores are emerging single-molecule sensors, known for its applications in nucleic acid sequencing,[23,24] or as general sensors of nucleic acids and proteins.[25] Nanopore based sensors are generally rapid, economic and can in principle be engineered to be portable.[26] Some specially engineered pores can even detect small molecules including D-glucose[27–35] or lactic acid.[36,37] *Mycobacterium smegmatis* porin A (MspA), a biological nanopore with a conical lumen geometry,[38] has a high sensing resolution in the discrimination of structurally similar small molecules.[39] With MspA, sensing of L-lactic acid[36] and D-glucose[29] has been previously carried out. However, simultaneous discrimination between chiral isomers of DL-lactic acid has never been demonstrated. Direct detection of endogenous DL-lactic acid, D-glucose and gluconic acid from serum samples has also never been shown.

Here, a sole phenylboronic acid (PBA) adapter is covalently attached to the constriction of the MspA nanopore. For simplicity, this chemically modified pore is referred to as MspA-90PBA (Methods). The success of mutation and modification can be confirmed by the sequencing results of corresponding plasmid DNA, gel electrophoresis results and characteristic current features observed during single channel recording. A complete workflow for nanopore serum analysis using MspA-90PBA is demonstrated (**Scheme 1**). Briefly, the serum sample is first ultrafiltration treated. To initiate nanopore analysis, the collected filtrate is directly added to the nanopore device to generate nanopore events. *Cis*-diols such as L-lactic acid, D-lactic acid, D-glucose and gluconic acid can form reversible borate esters with the PBA adapter of MspA-90PBA, reporting unique nanopore event features for identification. Assisted by a custom machine learning algorithm, different target compounds in real serum can be directly identified with a high accuracy. Although some interfering components in the serum sample may also react with PBA to produce events, their event features are fully distinguishable from the target events, acknowledging the high resolution of the MspA nanopore. To the best of our knowledge, direct and simultaneous nanopore identification of L-lactic acid, D-lactic acid, and D-glucose from real serum samples has never been reported previously. This strategy is fast and does not require complex sample separation. These results demonstrate the potential application of the nanopore sensor in medical diagnosis and provide inspirations for the development of point of care testing (POCT) devices.

2. Results and Discussion

2.1. Nanopore Identification of L-Lactic Acid in Blood Serum

To demonstrate the feasibility of this technique, the measurement was first performed with human serum reagent. To minimize the interferences caused by proteins in the serum, the serum was first added to an ultracentrifugation tube with a 3 kDa molecular weight cut off (MWCO) and then centrifuged at 3380 g for 20 min to collect the filtrate. Then, 100 µL filtrate was directly added to the *cis* chamber of the nanopore device.

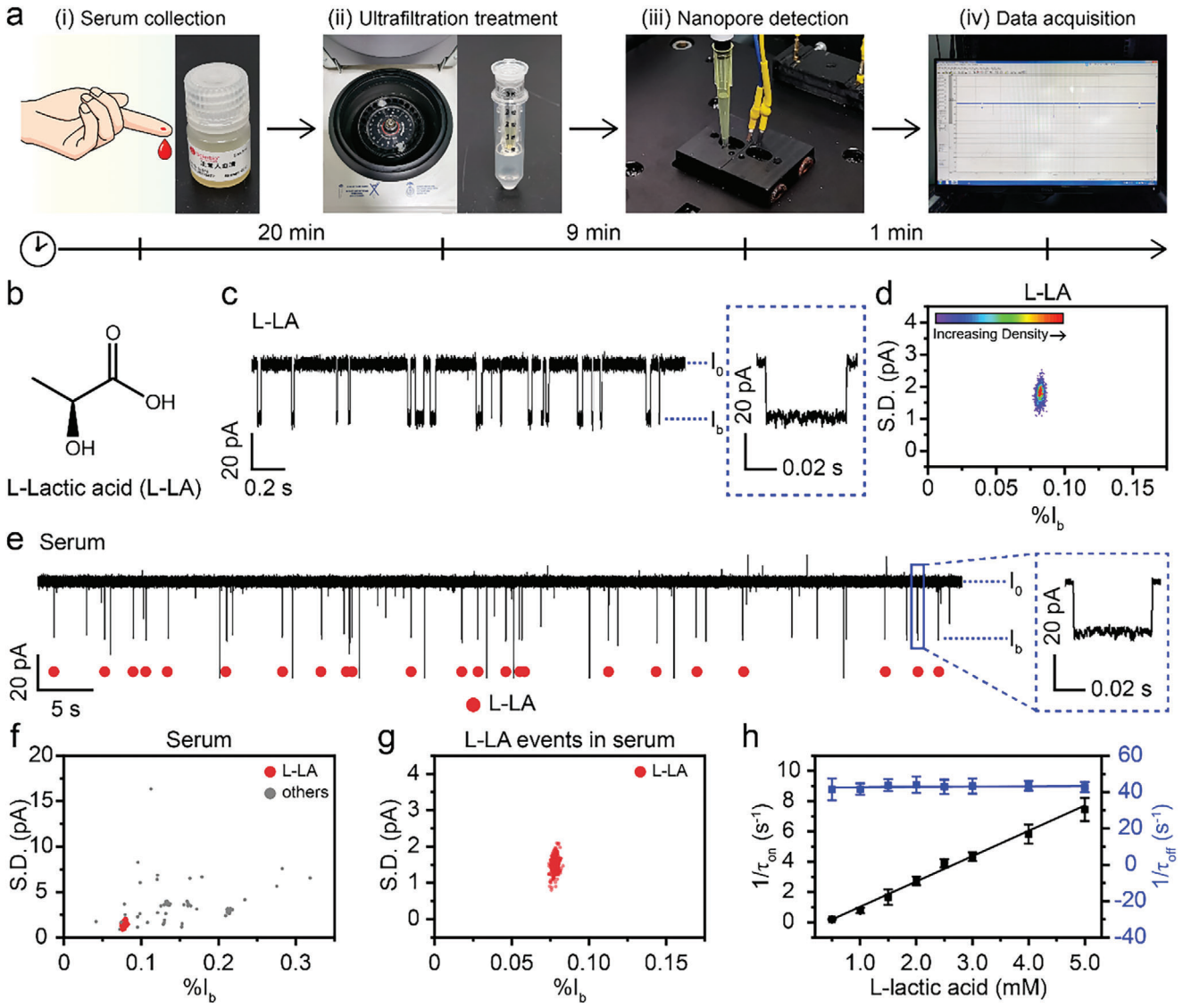

Figure 1. Nanopore identification of L-lactic acid in human blood serum. a) The demonstration of nanopore serum analysis workflow. Standard human serum (Solarbio Science & Technology, Beijing) was used for the demonstration. The serum was first ultracentrifuge treated to collect the filtrate. The filtrate was directly added to the *cis* chamber of the nanopore device to initiate the measurement. b) The chemical structure of L-lactic acid. c) A representative trace acquired with L-lactic acid using MspA-90PBA. A representative L-lactic acid event is shown in the blue dashed box. d) The event scatter plot of percentage blockage ($\%I_b$) versus standard deviation (*S.D.*) of L-lactic acid events. The scatter plot is color-coded by the local event density around each data point. A total of 3221 events are included in the plot. These events were extracted from a 20-min continually recorded trace and the final concentration of L-lactic acid was 2 mM. e) A representative trace acquired with 100 µL serum filtrate added to the *cis* chamber. Nanopore events of L-lactic acid were identified and labelled on the trace using the machine learning algorithm. The event in the blue dashed box is a zoomed-in demonstration of a L-lactic acid event in the trace. f) The scatter plot of $\%I_b$ versus *S.D.* of nanopore events acquired with serum. The scatter plot contains 575 events, which were extracted from a 40-minute continually acquired trace. The target (L-lactic acid) and interfering (others) events were discriminated by the One-Class SVM algorithm. g. The scatter plot of $\%I_b$ versus *S.D.* for L-lactic acid events acquired with serum. All interfering events were removed by the One-Class SVM algorithm. 497 events are included in the scatter plot. h) The concentration dependence plot of the reciprocal of mean inter-event interval ($1/\tau_{on}$) and the reciprocal of mean event dwell time ($1/\tau_{off}$) of L-lactic acid events. The error bars represent the average and standard deviation values derived from results acquired in three independent measurements (N = 3). All measurements were performed with MspA-90PBA in an electrolyte buffer of 1.5 M KCl, 100 mM MOPS, pH 7.0 (Methods). A +160 mV transmembrane potential was continually applied.

Immediately afterwards, successive appearance of nanopore events was observed (**Figure 1a**). It was speculated that the L-lactic acid (Figure 1b) in the serum might contribute to the generation of the majority of these nanopore events.

To confirm this hypothesis, nanopore measurements were also performed with pure L-lactic acid. With an MspA-90PBA inserted in the membrane (Methods), L-lactic acid, which was dissolved in a 0.9% NaCl solution, was directly added to the *cis* chamber. A transmembrane potential of +160 mV was continually

applied. Events generated by L-lactic acid are highly consistent in the event features (Figure 1c), appearing as a single type of nanopore events. To quantitatively describe event characteristics, major event features, including the inter-event interval (t_{on}), the event dwell time (t_{off}), the percentage blockade of nanopore events ($\%I_b$) and the standard deviation (*S.D.*), are defined in Figure S1 (Supporting Information). The event scatter plot of $\%I_b$ versus *S.D.* for L-lactic acid events demonstrate that only a single population of events were observed with L-lactic acid and the $\%I_b$ measures ≈0.08 (Figure 1d).

On the other side, during nanopore analysis of human serum (Figure 1a), multiple types of events were simultaneously observed (Figure 1e,f), suggesting that a variety of compounds in the serum can also report nanopore events. Based on the existing knowledge of the event features of L-lactic acid, a custom One-Class SVM algorithm, which serves for outlier analysis, was established (Figures S2 and S3, Supporting Information). Assisted by the algorithm, a cluster of events acquired with the serum were identified to be L-lactic acid. For demonstration, these identified events were considered as inlier events and were labelled on the trace (Figure 1e and Movie S1, Supporting Information). Events which fail to fit with the event features of L-lactic acid were however considered as outliers and were not labelled. A zoomed in demonstration of this trace is also shown in Figure S4 (Supporting Information). In the event scatter plot of $\%I_b$ versus *S.D.* of all events acquired with human serum, the events corresponding to L-lactic acid and all other outlier events are respectively marked. The event distribution of the L-lactic acid acquired with human serum (Figure 1g) is also highly consistent with that acquired with standard L-lactic acid (Figure 1d). Results acquired with three independent measurements were also simultaneously shown in Figure S5 (Supporting Information) and a high consistency of result is confirmed. In the concentration-dependence assay, the reciprocal of the mean inter-event interval ($1/\tau_{on}$) is linearly correlated with the L-lactic acid concentration, within the concentration range between 0.5–5 mM. While the reciprocal of the mean event dwell time ($1/\tau_{off}$) stays constant (Figure 1h; Figure S6 and Table S1, Supporting Information). These results suggest that the rate of event appearance can be used for quantitative analysis of L-lactic acid and a high dynamic range of measurement is shown. However, the event features of L-lactic acid are highly consistent and are independent of the L-lactic acid concentration, which guarantees the reliable sensing performance of this strategy.

Sensing of L-lactic acid was also performed with the M2 MspA mutant, which fails to have the PBA modification (Figure S7, Supporting Information). No nanopore events were observed, suggesting that the PBA modification plays a key role in the generation of L-lactic acid sensing events. The PBA adapter also plays a critical role by having a high specificity, which serves to reversibly react with only *cis*-diols in the serum. However, other compounds in the serum, which fail to have a *cis*-diol moiety, are in principle not detectable. On the other side, all outlier events (Figure 1f) detected from the serum may be from compounds in the serum which also have a *cis*-diol moiety. Acknowledging the high resolution of MspA, these outlier events are clearly distinguishable from that produced by the L-lactic acid. However, to the best of our knowledge, nanopore identification of L-lactic acid directly from human serum has never been reported before.

Though this sensing strategy is also suitable for direct analysis of serum however without any ultrafiltration treatment (Figure S8, Supporting Information), proteins naturally existed in the serum may be frequently trapped in the large vestibule to produce interfering events,[40,41] prohibiting efficient detection of L-lactic acid. This measurement interference is however minimized when the serum sample is ultracentrifuge treated prior to the nanopore measurement. The measurements were also carried out with different addition volumes of serum filtrate (Figure S9, Supporting Information), according to which a larger addition volume results in a clearly increased rate of event appearance. However, for consistency, if not otherwise stated, all following measurements were performed with 100 µL serum filtrate.

2.2. Simultaneous Identification of L-Lactic Acid and D-Lactic Acid in Serum Using Nanopore

D-lactic acid is the chiral isomer of L-lactic acid.[42] Endogenous D-lactic acid in the human body is usually produced by bacteria in the gastrointestinal tract. It is further converted to acetate and fatty acids by other microorganisms under normal circumstances. However, when the functions of gastrointestinal tract or intestinal barrier are impaired, D-lactic acid, which accumulates in the body, may enter the blood circulation, causing D-lactate acidosis.[2] As previously investigated, the increase of D-lactic acid level is observed in the blood of patients with short bowel syndrome or necrotizing enterocolitis.[43] Some diabetic patients may also report abnormal level of serum D-lactic acid.[44] Thus, direct sensing of D-lactic acid in serum is of significant clinical values. However, accurate quantification of D-lactic acid may be strongly interfered by its chiral isomer L-lactic acid in the serum.

The above demonstrated MspA-90PBA sensor is in principle suitable for both DL-lactic acid. Similar to that previously demonstrated with isomers of saccharides[29] and alditols,[45] the high resolution of MspA should also produce discriminable nanopore event features for the discrimination of DL-lactic acid. However, direct nanopore discrimination of DL-lactic acid has never been previously reported, to the best of our literature search results.

To demonstrate this, sensing of D-lactic acid was carried out at an identical condition previously used for L-lactic acid sensing (Figure S10 and Table S2, Supporting Information). Different from that of L-lactic acid, nanopore events of D-lactic acid systematically report much larger current fluctuations (**Figure 2**a,b; Figure S11, Supporting Information). This highly distinguishable event feature immediately allows for direct discrimination of DL-lactic acid. In the corresponding event scatter plot (Figure S12, Supporting Information), no event feature overlap is observed, suggesting that their discrimination is of no ambiguity at all. With training data respectively acquired with D- and L-lactic acid, a custom machine learning based classification model for the discrimination of DL-lactic acid events was also established (Figure S13, Supporting Information). When D-lactic acid and L-lactic acid were simultaneously sensed, the model can automatically identify DL-lactic acid events (Figure 2c). For demonstration, the identified DL-lactic acid events are also shown in the trace (Figure 2d). To this end, simultaneous sensing and discrimination of DL-lactic acid is successfully demonstrated.

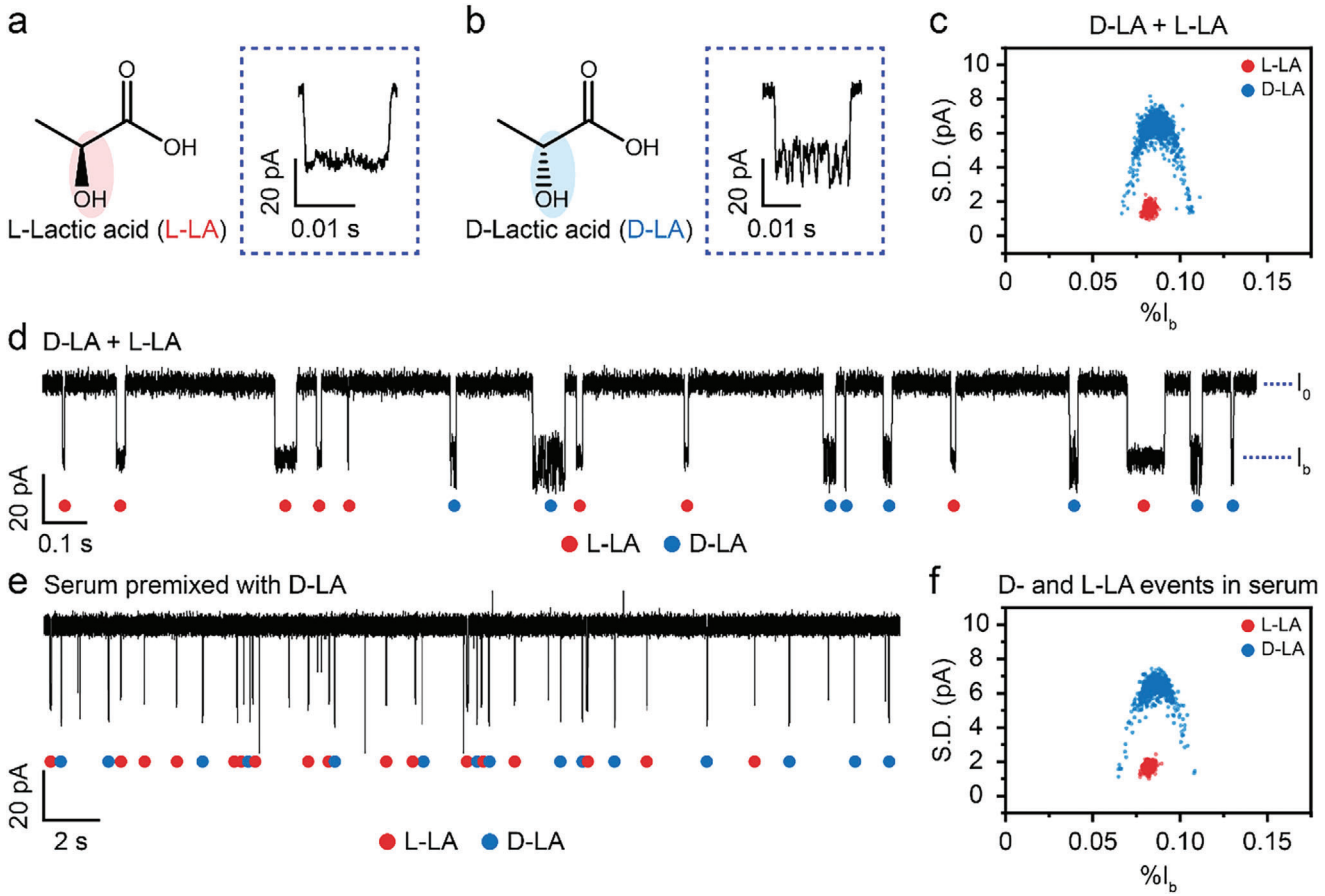

Figure 2. Nanopore discrimination of L- and D-lactic acid in blood serum. a,b) The chemical structures of L-lactic acid (a) and D-lactic acid (b). Their representative events are demonstrated to the right. The event features of L- and D-lactic acid are highly distinguishable based on their event noise differences. c) The event scatter plot of $\%I_b$ versus *S.D.* for nanopore events acquired with a mixture of L- and D-lactic acid. The L- and D-lactic acid were simultaneously added to *cis* with a final concentration of 2 mM for each component. The scatter plot contains 2231 events, which were extracted from a 20-minute continually recorded trace. Two populations of events, respectively corresponding to events of L- and D-lactic acid, were identified. d) The representative trace acquired with the mixture of L- and D-lactic acid. All events were identified by a custom machine learning algorithm and colour labelled accordingly. e) A representative trace acquired with human serum premixed with D-lactic acid. D-lactic acid was first added to the serum to reach a 3 mM final concentration. The serum was then ultrafiltration treated. 100 µL filtrate was collected and added to *cis* to initiate the measurement. The target and interfering events were identified by the One-Class SVM algorithm and the event identities were accordingly labelled on the trace. f) The event scatter plot of $\%I_b$ versus *S.D.* for L- and D-lactic acid events acquired with serum premixed with D-lactic acid. The interfering events were computationally removed by corresponding machine learning algorithms. The scatter plot contains 1205 events, which were extracted from a 40-minute continually recorded trace. All measurements were performed with MspA-90PBA in an electrolyte buffer of 1.5 M KCl, 100 mM MOPS, pH 7.0 (Methods). A +160 mV transmembrane potential was continually applied.

To show sensing of D-lactic acid in a human serum environment, mimicking the diagnostic criteria of D-lactic acidosis (D-lactic acid level ≥3 mM in serum),[46] the standard human serum sample was added with D-lactic acid to reach a 3 mM final concentration and gently oscillated at 37 °C for 20 minutes to reach a homogenous distribution. Afterward, the serum was ultracentrifuge treated to collect the ultrafiltrate. During single channel recording with MspA-90PBA, immediately after the addition of 100 µL ultrafiltrate, successive appearance of corresponding nanopore events was immediately observed (Figure 2e).

In the zoomed-in view of the trace, the differences of events between D-lactic acid and L-lactic acid can also be clearly observed (Figure S14, Supporting Information). The scatter plot of $\%I_b$ versus *S.D.* for these nanopore events were plotted, and events generated by D-lactic acid and L-lactic acid were color-coded accordingly (Figure 2f). Similar measurements were also performed in three independent measurements and a high consistency of result is reported (Figure S15, Supporting Information).

The above results demonstrate that the engineered MspA nanopore can simultaneously discriminate between DL-lactic acid. This sensing capacity is also demonstrated in a human serum environment, suggesting the immediate clinical value of this nanopore sensing strategy. Compared with conventional enzymatic methods,[17,18] this nanopore sensing method does not require the lactate dehydrogenase during sensing of D-lactic acid. Acknowledging the high resolution of the nanopore which immediately resolves chiral isomers, it also doesn't require any chiral separation. The measurement only needs 100 µL of input serum, which is potentially advantageous for clinical diagnosis.

2.3. Identification of D-Glucose in Blood Serum by Nanopore

D-Glucose, the energy source for almost all living organisms, widely exists in a variety of biological fluids and tissues. The glucose levels in body fluids are associated with many pathologic conditions, including cancer, diabetes and obesity.[7,8] The evaluation of the blood glucose level has a great significance in the evaluation of the human health condition. The conventional analytical methods for glucose are mainly based on glucose oxidase, glucose dehydrogenase or hexokinase, such as enzymatic spectrophotometry and enzymatic colorimetry.[16] By attaching these enzymes to nanomaterials, such as carbon nanotubes, graphene quantum dots or hydrogels, the applications of the enzymatic detection system are further expanded.[15] Several non-enzymatic methods for glucose sensing, such as HPLC,[47] aptamer[22] and direct electro-oxidation of glucose by electrodes,[48] were also developed.

With nanopores, glucose sensing was previously performed by trapping glucose oxidase in the lumen of a large-size nanopore.[28] However, this indirect sensing strategy is limited by the specificity of the enzyme substrate, which fails to sense any compounds that are in principle not substrates of the trapped enzyme. The observed nanopore events only reflect binding kinetics of the enzyme instead of the bound substrate. Thus, the reported nanopore event features can't perform simultaneous sensing of multiple compounds in the same assay. On the other side, nanopore D-glucose sensing has also been carried out by phenylboronic acid modified α-Hemolysin (α-HL)[27] and MspA nanopores.[29] However, direct nanopore D-glucose sensing from human serum was not carried out due to the complexity of the serum environment. With the development of corresponding machine learning algorithms and the existing knowledge of nanopore event signatures of DL-lactic acids (Figure 2), we anticipate that simultaneous sensing of DL-lactic acid and D-glucose should be carried out solely using MspA-90PBA.[29]

Due to the complexity of D-glucose configurations in an aqueous solution, nanopore sensing of D-glucose simultaneously reports multiple types of events (**Figure 3**a,b; Figures S16 and S17, Supporting Information). According to the scatter plot of $\%I_b$ versus *S.D.* results acquired with D-glucose (Figure 3c), five major populations of events were observed by MspA-90PBA. For clarity, different types of D-glucose events were also marked with Roman numerals on the scatter plot, respectively corresponding to the representative events in Figure 3b.

The inherent D-glucose concentration in human serum is ≈5.5 mM.[49] To more efficiently show nanopore events of D-glucose in a human serum environment, the serum sample was further added with D-glucose to reach a 11 and 22 mM final concentration. Specifically, the 11 and 22 mM D-glucose concentrations respectively correspond to the diagnosis criteria for diabetes and severe hyperglycemia.[50,51] Each serum sample was identically treated with ultracentrifugation to collect the filtrate. In separate measurements, 100 µL filtrate was added to the nanopore device and single channel measurement was continually recorded for 40 min. In the produced event scatter plot of $\%I_b$ versus *S.D.*, nanopore events of D-glucose were clearly seen from the normal human serum sample. Events corresponding to L-lactic acid were also simultaneously observed (Figure 3d), confirming our hypothesis that simultaneous sensing of D-glucose and L-lactic acid directly using human serum samples could be achieved solely by MspA-90PBA. It is also demonstrated that, more D-glucose events were observed with the serum samples however with added D-glucose, indicating that the rate of event appearance is strongly correlated with the analyte concentration (Figure 3e,f) and the current sensitivity of the measurement strategy is sufficient for the diagnosis of diabetes and severe hyperglycemia.

With the existing knowledge of the nanopore event features of D-glucose and L-lactic acid, a custom machine learning algorithm was also established (Figure S18, Supporting Information). The machine learning algorithm was used for the classification of D-glucose and L-lactic acid events acquired with the serum samples (Figure 3d). This phenomenon is also consistently observed based on results produced in three independent measurements (Figure 3g; Figures S19–S21, Supporting Information). A representative trace acquired with the serum sample containing a 22 mM D-glucose concentration is shown in Figure 3h. Nanopore events of L-lactic acid and D-glucose can be identified by a custom machine learning algorithm and the identified events are labelled on the trace. To show more details, a zoomed in view of this trace is also provided in Figure S22 (Supporting Information). All above demonstrations have confirmed that this nanopore platform can directly and simultaneously identify D-glucose and L-lactic acid in human serum, which has the potential of clinical diagnosis of human diseases, such as diabetes,[8] lactic acidosis[2,3] and diabetic lactic acidosis[52] solely using the same system.

The endogenous D-lactic acid concentration in human serum is ≈0.01 mM.[53] To further show the resolution of this technique to simultaneously identify DL-lactic acid and D-glucose, standard human serum was added with D-lactic acid and D-glucose. This specially prepared human serum sample was identically ultracentrifuge treated to collect the ultrafiltrate. During nanopore analysis (Methods), 100 µL filtrate was added to the nanopore device and single channel measurement was continually recorded for 40 min.

With the input of standard event features of DL-lactic acid and D-glucose (Table S3, Supporting Information), a machine learning algorithm was established and immediately used for the analysis of this serum sample (Figure S23, Supporting Information). The event scatter plot of $\%I_b$ versus *S.D.* for events acquired with this prepared serum was shown in **Figure 4**a, from which events of DL-lactic acid and D-glucose are clearly seen. Generally, the event distribution is highly consistent with results acquired with pure compound of DL-lactic acid (Figure S3 and S11, Supporting Information) and D-glucose (Figure S17, Supporting Information). Here, all events were classified by the custom machine learning algorithm (Figure S23, Supporting Information) and labelled according to the prediction results. Details of data analysis and results separately acquired with three independent measurements are summarized in Figure S24 (Supporting Information). A representative trace acquired at this condition is also shown in Figure 4b, in which the events corresponding to DL-lactic acid and D-glucose are clearly labelled according to the machine learning prediction results. To show more event details, a zoomed in view of this trace is also provided (Figure S25, Supporting Information). On the other side, direct nanopore analysis of human serum without any D-lactic acid addition results in the detection of 0–3 D-lactic acid events in a

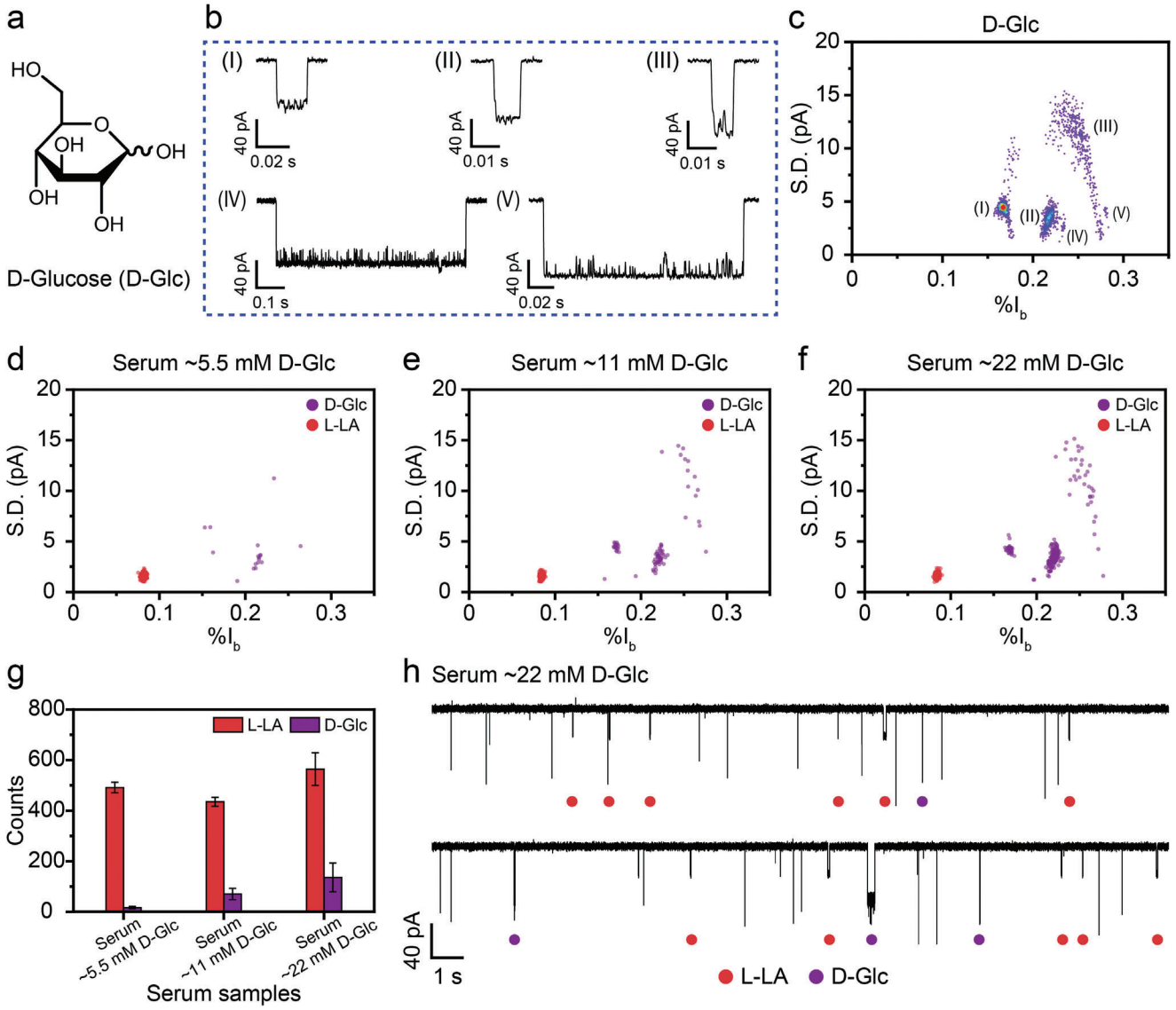

Figure 3. Nanopore identification of D-glucose in blood serum. a) The chemical structure of D-glucose. b) Representative nanopore events of D-glucose. D-Glucose could bind to PBA with varying configurations, resulting in five event types, respectively marked with Roman numerals. c) The scatter plot of $\%I_b$ versus *S.D.* for nanopore events acquired with D-glucose. The event types of D-glucose are respectively labelled in the scatter plot. D-Glucose was added to *cis* with a final concentration of 60 mM. The scatter plot contains 1655 events, extracted from a 20-minute continually recorded trace. d–f) The scatter plot of $\%I_b$ versus *S.D.* for nanopore events acquired with serum premixed with different concentrations of D-glucose. The natural concentration of D-glucose in blood serum was ≈5.5 mM (d), and serum samples with final concentrations of 11 mM (e) and 22 mM (f) were prepared by further addition of D-glucose to the serum. The scatter plots (d–f) respectively contain 485, 495, and 695 events, which were respectively extracted from 40-minute traces acquired at each condition. Only D-glucose and L-lactic acid events were retained in the scatter plots for further analysis (Figures S19–S21, Supporting Information). g) The corresponding counts of D-glucose and L-lactic acid events for different blood serum samples (d-f). h) A representative trace acquired with serum with 22 mM D-glucose. All measurements were performed with MspA-90PBA in an electrolyte buffer of 1.5 M KCl, 100 mM MOPS, pH 7.0 (Methods). A +160 mV transmembrane potential was continually applied. All serum samples were ultrafiltration treated. 100 µL filtrates were added to the *cis* chamber to initiate the measurements for each condition.

continuous 40 min measurements (Figure S26, Supporting Information). This result suggests that direct detection of endogenous D-lactic acid from human serum is achievable but limited by the sensing efficiency of the current sensing configuration, which may be further optimized using a higher density of nanopore arrays or a miniaturized measurement chamber. Despite the low level of D-lactic acid in human serum, the physiological level of L-lactic acid and D-glucose is enough to be detected by MspA-90PBA, suggesting immediate corresponding healthcare applications.

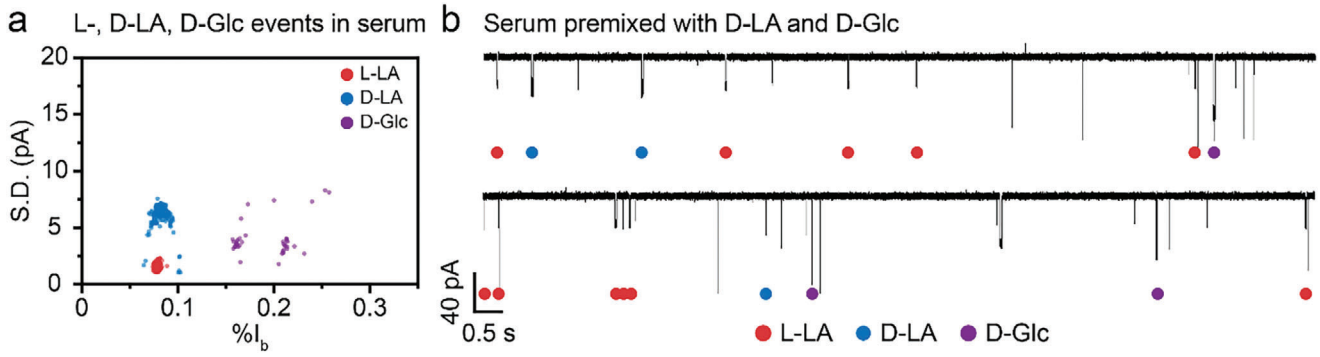

Figure 4. Simultaneous identification of L-, D-lactic acid and D-glucose in blood serum. The measurements were performed using MspA-90PBA in an electrolyte buffer of 1.5 M KCl, 100 mM MOPS, pH 7.0 (Methods). The serum was added with D-lactic acid and D-glucose to have a final concentration of 1 mM D-lactic acid and 11 mM D-glucose. To initiate the measurement, 100 µL ultrafiltrate of serum was added to the *cis* chamber. A transmembrane potential of +160 mV was continually applied. a) The scatter plot of $\%I_b$ versus *S.D.* for nanopore events acquired with serum added with D-lactic acid and D-glucose. Only L-, D-lactic acid and D-glucose events were retained on the scatter plots for further analysis (Figure S24, Supporting Information). The scatter plot contains 811 events, which were extracted from a 40-minute continually recorded trace. b) A representative trace acquired with the serum containing L-, D-lactic acid and D-glucose events. The events were automatically identified by the machine learning algorithm and labelled on the trace. Events generated by other interfering components in the blood serum were identified but removed without further analysis.

2.4. Nanopore Identification of Animal Blood Serum

All above measurements tested with human serum are also in principle suitable for the analysis of animal blood. To show its feasibility, different animal sera were ultracentrifuge treated as before to collect the ultrafiltrate. In each measurement, a 100 µL ultrafiltrate of the serum was added to the nanopore device to initiate the measurement. According to the event scatter plot results, all animal serum samples reported events of DL-lactic acid and D-glucose (**Figure** 5a–e).

However, a previously unidentified event type was clearly identified in the chicken serum. Based on literature search and event feature comparison, this newly identified event type was later confirmed to be gluconic acid (Figure S27, Supporting Information). Gluconic acid is beneficial to maintain the activities of various digestive enzymes by regulating the pH of the gastrointestinal tract. In breeding industry, it is usually used as a feed additive or produced due to the addition of glucose oxidase to the fodder.[11,12] To minimize interferences caused by non-clustered events and outliers, a custom machine learning algorithm for the analysis of animal serum was also developed (Figure S28, Supporting Information).

The consistency of nanopore measurement results was also evaluated by results acquired with three independent measurements (Figures S29–S33, Supporting Information). To show more details of events, zoomed in views of traces acquired with the animal serum are also provided (Figures S34–S38, Supporting Information). Though measured at an identical measurement condition, the levels of DL-lactic acid, D-glucose and gluconic acid are significantly different for serum from different animals (Figure 5f). L-lactic acid is the important metabolite of glycolysis in organisms,[3] and therefore they all have high levels of L-lactic acid in their serum. Chicken serum contains a large amount of gluconic acid compared to other animals, which may be due to the fact that glucose oxidase is mainly applied in the poultry industries and can significantly promote animal growth.[11] In addition, large amounts of D-lactic acid were found in chicken serum, which may be generated by bacteria in their digestive tract.[54] However, only few D-lactic acid events were detected in human serum sensing (0-3 events in a 40-minute continually recording). For goat, bovine, horse and rabbit serum, only a low level of D-lactic acid, D-glucose and gluconic acid were detected.

To this end, we have successfully demonstrated direct analysis of the serum from human and a variety of animals solely using MspA-90PBA. Different levels of DL-lactic acid, D-glucose and gluconic acid were clearly identified from the serum. For different sources of the serum, the levels of different above-mentioned compounds were clearly different, suggesting that a nanopore measurement can easily discriminate between serum samples collected from different living organisms. However, direct nanopore analysis of serum samples from different species have never been previously reported. The nanopore signatures of D-lactic acid and gluconic acid were also not previously known, prior to this work. The PBA adapter of MspA-90PBA also serves to minimize interferences caused by other serum metabolites which fail to show an affinity to the PBA (Figure S39, Supporting Information). For *cis*-diols that are not of a sufficiently high concentration in the serum, the rate of event appearance will be too low for efficient detection.

The limit of detection in this work is defined as the minimum input analyte concentration, with which at least 5 events could be detected within a continuous 10-minute measurement (Table S4, Supporting Information). The L-lactic acid in the blood is usually between 0.5 and 2.2 mM, and can transiently reach 15 mM after vigorous exercise,[3] indicating that the L-lactic acid is immediately detectable by this system, without any need of sample enrichment. On the other side, the physiology concentration of D-glucose is between 4 and 7 mM,[55] which is also within the dynamic range of sensing of this system.

For a quick demonstration, all measurements were carried out with an Axon 200B patch clamp amplifier paired with an Axon 1550B digitizer. In principle, all above measurements can also be demonstrated in a highly portable nanopore device, similar to the size of a MinION sequencer[56] to show its portability. The ultracentrifugation operation may as well be carried out by a battery

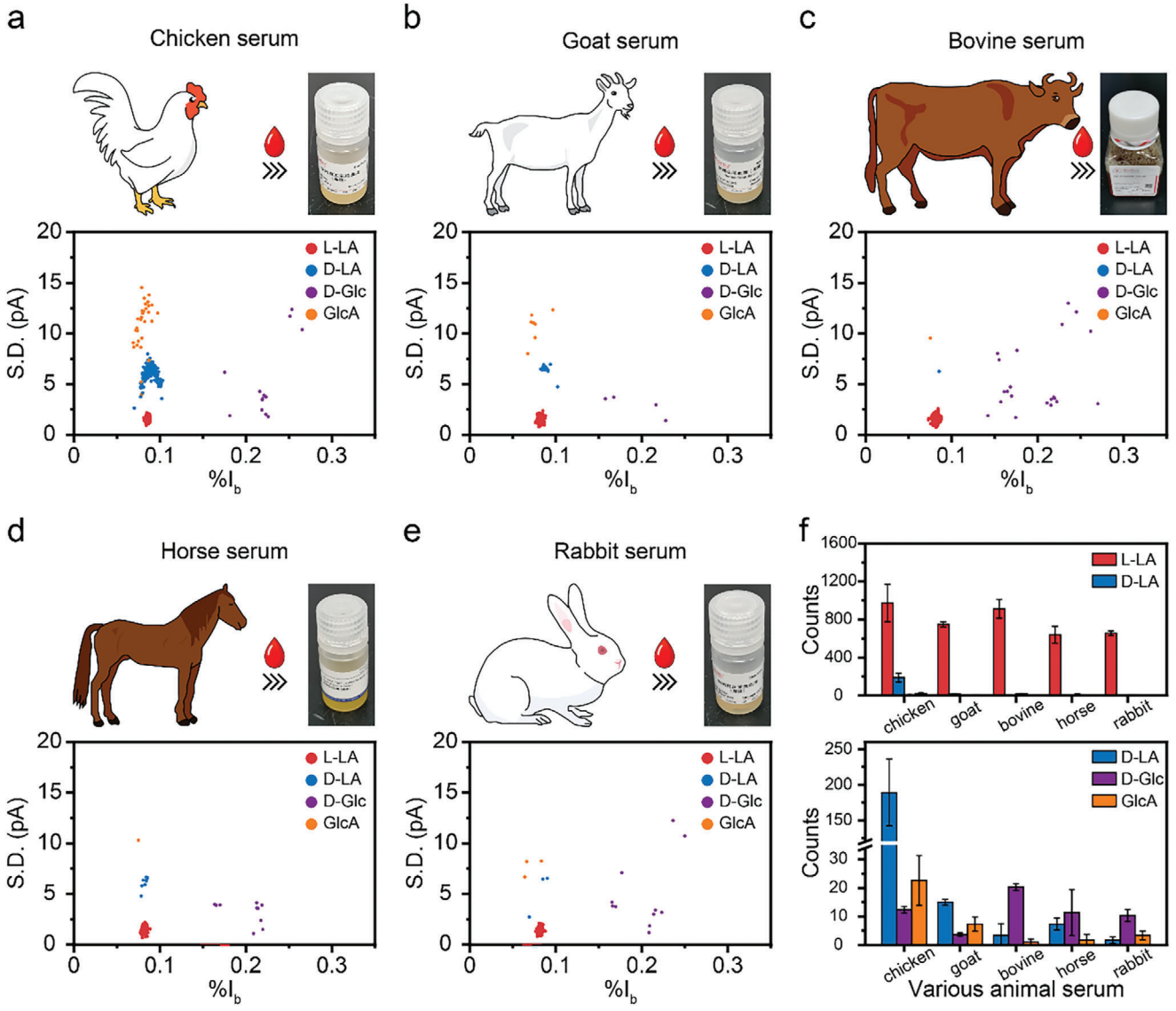

Figure 5. Nanopore analysis of animal blood serum. The measurements were performed using MspA-90PBA in an electrolyte buffer of 1.5 M KCl, 100 mM MOPS, pH 7.0 (Methods). To initiate the measurement, the sera of different animals were ultrafiltration treated. The filtrate was collected and directly added to *cis* to initiate the measurement. A +160 mV transmembrane potential was continually applied. a–e) Top: Cartoon of animals and the corresponding blood serum standards obtained from the animals. Bottom: The scatter plot of $\%I_b$ versus *S.D.* for nanopore events respectively acquired from chicken (a), goat (b), bovine (c), horse (d) and rabbit (e). Only L-, D-lactic acid, D-glucose and gluconic acid events were retained in the scatter plots. All other interfering events were identified by the one-class SVM algorithm and removed prior to further analysis. The scatter plot contains 1044, 752, 1025, 676, and 699 events, which were respectively extracted from corresponding traces of 20-minute duration. f) Top: The histograms of the event counts for L-, D-lactic acid, D-glucose and gluconic acid in the serum of different animals, as described in (a–e). Bottom: The zoomed-in view of histograms of the event counts for D-lactic acid, D-glucose and gluconic acid acquired from serum of different animals. The error bars represent the average and standard deviation values obtained from results of three independent measurements (N = 3).

powered mini-centrifuge. The nanopore measurements may as well be carried out in a miniatured nanopore chamber accompanied with a large array of nanopores to further improve its limit of detection as well.

3. Conclusion

Nanopore identification of L-lactic acid, D-lactic acid, D-glucose and gluconic acid was simultaneously performed using a PBA modified MspA nanopore. Acknowledging the high resolution of MspA, all above compounds report highly distinguishable event features, allowing for simultaneous analysis of all above analytes in the same system. Nanopore discrimination of DL-lactic acid requires no need of sample separation, demonstrating a simplicity over conventional analytical methods. To assist result analysis, a custom machine learning algorithm was developed and a high accuracy was reported. All above compounds may simultaneously exist in the blood of human and animals. Acknowledging

the high resolution of the pore and the selectivity gained by the PBA adapter, this system can be directly used for the analysis of serum of human and different animals, suggesting its potential in the diagnosis of diseases such as lactic acidosis,[2,3] diabetes[8] and diabetic lactic acidosis[52] and applications in agriculture science or breeding industry. This sensing strategy is generally simple, rapid and economic. Though not demonstrated in this paper, this sensing strategy is in principle also suitable to be integrated into a highly portable device to show its POCT applications in the future.

4. Experimental Section

Nanopore Preparations: $(N90C)_1(M2)_7$ was a hetero-octameric MspA assembly, containing one N90C MspA-H6 monomer and seven M2 MspA-D16H6 monomers.[29] To prepare the hetero-octameric pore $(N90C)_1(M2)_7$, the genes respectively coding for MspA-D16H6 and N90C MspA-H6 were custom synthesized and introduced to a pETDuet-1 plasmid by Genscript (New Jersey, U.S.). The generated plasmid was then transformed to *E. coli* strain BL21(DE3) plysS competent cells and the corresponding genes were expressed. The expression products were purified by nickel affinity chromatography and further separated by polyacrylamide gel electrophoresis (PAGE). The band corresponding to $(N90C)_1(M2)_7$ protein was excised from the gel and the corresponding protein was recovered. The prepared $(N90C)_1(M2)_7$ protein was either used immediately or stored at −80 °C for long term storage. The $(N90C)_1(M2)_7$ contains a sole cysteine residue that can be used for specific chemical linkage, facilitating further nanopore functionalization.

The MspA-90PBA nanopores were prepared by the maleimide-thiol coupling reaction between the sole cysteine residue of $(N90C)_1(M2)_7$ and the 3-(maleimide) Phenylboronic acid (MPBA). To perform the pore modification, 2 µL $(N90C)_1(M2)_7$ protein, 1 µL MPBA (500 mM, in DMSO) and 20 µL measuring buffer (1.5 M KCl, 100 mM MOPS, pH 7.0) were mixed and incubated at room temperature for 10 minutes. The prepared MspA-90PBA was immediately used for single channel recording.

M2 MspA (D93N/D91N/D90N/D118R/D134R/E139K) was a homogeneous octameric nanopore.[57] The M2 MspA nanopores do not contain any cysteine residues and cannot be further functionalized by the maleimide-thiol coupling reaction. For this reason, the M2 MspA serves as a negative control in the evaluation of the functional role of the PBA adapter.

Nanopore Measurements: The measuring device consists of two identical chambers, each filled with 500 µL measuring buffer. The two chambers were separated by a thin Teflon film containing an aperture with a 100 µm diameter. A pair of Ag/AgCl electrodes, which were electrically connected to the patch clamp amplifier, were inserted in the chambers, in contact with the buffers. Generally, the grounded electrode was defined as *cis*. Whereas, its opposing electrode was defined as *trans*. Nanopores were added to the *cis* chamber. The nanopore can spontaneously insert into the lipid bilayer. When a single nanopore was inserted, the electrolyte buffer in the *cis* chamber was immediately exchanged to avoid further nanopore insertions. Single channel recording was performed by an Axopatch 200B patch clamp amplifier paired with a Digidata 1550B digitizer (Molecular Devices, UK). Nanopore traces were sampled at 25 kHz and low-pass filtered with a corner frequency of 1 kHz. All measurements were performed at room temperature (21±2 °C). To ensure the consistency of measurements, all measuring conditions were described above, unless otherwise stated.

Data Analysis: All nanopore events were detected by the Single-Channel Search function in Clampfit 10.7 (Molecular Devices, UK). Event feature parameters, including $\%I_b$, *S.D.*, t_{off}, *skew*, *kurt*, $\%I_{max}$ and $\%I_{min}$, were extracted by a custom MATLAB program (Figures S2 and S13, Supporting Information). To minimize interferences caused by non-clustered events, events which exceed the average blocking current with a ±3 times standard deviation were ignored during statistics. Nanopore events with t_{off} less than 5 ms were also ignored. All statistics and plotting operations, including histogram plots and curve fitting, scatter plots, etc., were performed in Origin 2021 (Origin Lab).

The machine learning algorithm was developed using the Classification Learner toolbox in MATLAB R2019b (MathWorks, US). One-Class SVM was a machine learning algorithm for outlier analysis. The training datasets for outlier analysis of L-lactic acid, L-lactic acid and D-lactic acid, L-lactic acid and D-glucose, as well as L-, D-lactic acid and glucose in serum, were composed of standard events for the corresponding analytes, respectively. Each class of events contain 3000 events. Briefly, $\%I_b$, *S.D.*, t_{off}, *skew*, *kurt*, $\%I_{max}$ and $\%I_{min}$ were employed as event features for outlier analysis. For L-lactic acid, D-lactic acid, and D-glucose, the parameter "OutlierFraction" was set to 0.002, 0.002, and 0.01, respectively. Different One-Class SVM models were trained by the corresponding training datasets, and the classification models established in MATLAB were used for further event discrimination. The One-Class SVM model automatically judges whether an event belongs to any previously trained event type, so that the event was judged as an inlier/outlier event. The previously trained classification model was used for further event prediction (Figure S13, Supporting Information).

Nanopore Analysis of Blood Serum: Prior to nanopore measurements, all serum samples were stored at −20 °C and slowly thawed at 4 °C. 200 µL serum was added to an ultrafiltration tube (3 kDa, 0.5 mL) and centrifuged at 3380 g for 20 min. Subsequently, 100 µL serum filtrate was directly added to *cis* chamber. A +160 mV potential was continually applied.

At this point, the *cis* chamber was filled with 100 µL serum and a 400 µL electrolyte buffer, while the *trans* chamber was filled with a 500 µL electrolyte buffer. Therefore, to balance the influence of the ionic strength on the measurement, all standard compounds used in this study were dissolved in an isotonic 0.9% NaCl solution and added to the *cis* chamber at a final volume of 100 µL. For premixed serum samples, D-glucose and D-lactic acid were added to the serum at the desired concentrations and slowly oscillated at 37 °C for 20 min. The pre-treatment and nanopore detection of these serum samples were kept consistent throughout this manuscript, if not otherwise stated.

Supporting Information

Supporting Information is available from the Wiley Online Library or from the author.

Acknowledgements

W.J. and Y.O. contributed equally to this work. This project was funded by National Natural Science Foundation of China (Grant No. 22225405, No. 31972917), National Key Research and Development Program of China (Grant No. 2022YFA1304602), the Fundamental Research Funds for the Central Universities (Grant No.020514380257), Programs for high-level entrepreneurial and innovative talents introduction of Jiangsu Province (individual and group program), Excellent Research Program of Nanjing University (Grant No. ZYJH004), the China Postdoctoral Science Foundation (Grant No. 2022M721554, No. 2023T160300, to W.D.J), Jiangsu Funding Program for Excellent Postdoctoral Talent (Grant No. 2023ZB643, to W.D.J).

Conflict of Interest

The authors declare no conflict of interest.

Data Availability Statement

The data that support the findings of this study are available from the corresponding author upon reasonable request.

Keywords

blood serum, DL-lactic acid, glucose, gluconic acid, Mycobacterium smegmatis porin A, single-molecule detection

Received: May 7, 2024
Revised: May 30, 2024
Published online: June 12, 2024

[1] X. Li, Y. Yang, B. Zhang, X. Lin, X. Fu, Y. An, Y. Zou, J.-X. Wang, Z. Wang, T. Yu, *Signal Trans. Target. Ther.* **2022**, *7*, 305.
[2] C. Petersen, *Nutr. Clin. Prac.* **2005**, *20*, 634.
[3] J. A. Kraut, N. E. Madias, *N. Engl. J. Med.* **2014**, *371*, 2309.
[4] N. Nikolaus, B. Strehlitz, *Microchim. Acta* **2008**, *160*, 15.
[5] Y. Wang, J. Wu, M. Lv, Z. Shao, M. Hungwe, J. Wang, X. Bai, J. Xie, Y. Wang, W. Geng, *Front. Bioeng. Biotechnol.* **2021**, *9*, 612285.
[6] M. Rigoulet, C. L. Bouchez, P. Paumard, S. Ransac, S. Cuvellier, S. Duvezin-Caubet, J. P. Mazat, A. Devin, *Biochim. et Biophys. Acta (BBA) – Bioenerg.* **2020**, *1861*, 148276.
[7] N. Hay, *Nat. Rev. Cancer* **2016**, *16*, 635.
[8] T. V. Rohm, D. T. Meier, J. M. Olefsky, M. Y. Donath, *Immunity* **2022**, *55*, 31.
[9] R. DeFronzo, G. A. Fleming, K. Chen, T. A. Bicsak, *Metabolism* **2016**, *65*, 20.
[10] J. Lu, G. A. Zello, E. Randell, K. Adeli, J. Krahn, Q. H. Meng, *Clin. Chim. Acta* **2011**, *412*, 286.
[11] Z. Liang, Y. Yan, W. Zhang, H. Luo, B. Yao, H. Huang, T. Tu, *Crit. Rev. Biotechnol.* **2023**, *43*, 698.
[12] P. Biggs, C. M. Parsons, *Poultry Sci.* **2008**, *87*, 2581.
[13] F. Alam, S. RoyChoudhury, A. H. Jalal, Y. Umasankar, S. Forouzanfar, N. Akter, S. Bhansali, N. Pala, *Biosens. Bioelectron.* **2018**, *117*, 818.
[14] G. Rattu, N. Khansili, V. K. Maurya, P. M. Krishna, *Environ. Chem. Lett.* **2021**, *19*, 1135.
[15] V. B. Juska, M. E. Pemble, *Sensors* **2020**, *20*, 6013.
[16] A. L. Galant, R. C. Kaufman, J. D. Wilson, *Food Chem.* **2015**, *188*, 149.
[17] C.-M. Chen, S.-M. Chen, P.-J. Chien, H.-Y. Yu, *J. Pharm. Biomed. Anal.* **2015**, *116*, 150.
[18] T. Satomura, J. Hayashi, H. Sakamoto, T. Nunoura, Y. Takaki, K. Takai, H. Takami, T. Ohshima, H. Sakuraba, S.-I. Suye, *J. Biosci. Bioeng.* **2018**, *126*, 425.
[19] R. B. Brandt, S. A. Siegel, M. G. Waters, M. H. Bloch, *Anal. Biochem.* **1980**, *102*, 39.
[20] M. Adeel, M. M. Rahman, I. Caligiuri, V. Canzonieri, F. Rizzolio, S. Daniele, *Biosens. Bioelectron.* **2020**, *165*, 112331.
[21] H. Henry, N. Marmy Conus, P. Steenhout, A. Béguin, O. Boulat, *Biomed. Chromatogr.* **2012**, *26*, 425.
[22] P.-J. J. Huang, J. Liu, *Angew. Chem., Int. Ed.* **2023**, *62*, 202212879.
[23] E. A. Manrao, I. M. Derrington, A. H. Laszlo, K. W. Langford, M. K. Hopper, N. Gillgren, M. Pavlenok, M. Niederweis, J. H. Gundlach, *Nat. Biotechnol.* **2012**, *30*, 349.
[24] D. R. Garalde, E. A. Snell, D. Jachimowicz, B. Sipos, J. H. Lloyd, M. Bruce, N. Pantic, T. Admassu, P. James, A. Warland, M. Jordan, J. Ciccone, S. Serra, J. Keenan, S. Martin, L. McNeill, E. J. Wallace, L. Jayasinghe, C. Wright, J. Blasco, S. Young, D. Brocklebank, S. Juul, J. Clarke, A. J. Heron, D. J. Turner, *Nat. Methods* **2018**, *15*, 201.
[25] Y.-L. Ying, Z.-L. Hu, S. Zhang, Y. Qing, A. Fragasso, G. Maglia, A. Meller, H. Bayley, C. Dekker, Y.-T. Long, *Nat. Nanotechnol.* **2022**, *17*, 1136.
[26] W. Jia, Y. Ouyang, S. Zhang, X. Du, P. Zhang, S. Huang, *Nano Lett.* **2023**, *23*, 9437.
[27] W. J. Ramsay, H. Bayley, *Angew. Chem., Int. Ed.* **2018**, *57*, 2841.
[28] N. S. Galenkamp, M. Soskine, J. Hermans, C. Wloka, G. Maglia, *Nat. Commun.* **2018**, *9*, 4085.
[29] S. Zhang, Z. Cao, P. Fan, Y. Wang, W. Jia, L. Wang, K. Wang, Y. Liu, X. Du, C. Hu, P. Zhang, H.-Y. Chen, S. Huang, *Angew. Chem., Int. Ed.* **2022**, *61*, 202203769.
[30] S. Zhao, Y.-B. Zheng, S.-L. Cai, Y.-H. Weng, S.-H. Cao, J.-L. Yang, Y.-Q. Li, *Electrochem. Commun.* **2013**, *36*, 71.
[31] M. Yang, C. Ma, S. Ding, Y. Zhu, G. Shi, A. Zhu, *Anal. Chem.* **2019**, *91*, 14029.
[32] D. Wang, G. Qi, Y. Zhou, H. Li, Y. Zhang, C. Xu, P. Hu, Y. Jin, *Chem. Commun.* **2020**, *56*, 5393.
[33] T. Zheng, Y. Zhu, A. Zhu, *Electroanalysis* **2022**, *34*, 326.
[34] R.-J. Yu, Q. Li, S.-C. Liu, H. Ma, Y.-L. Ying, Y.-T. Long, *Nanoscale* **2023**, *15*, 7261.
[35] R. A. S. Nascimento, R. E. Özel, W. H. Mak, M. Mulato, B. Singaram, N. Pourmand, *Nano Lett.* **2016**, *16*, 1194.
[36] W. Jia, C. Hu, Y. Wang, Y. Gu, G. Qian, X. Du, L. Wang, Y. Liu, J. Cao, S. Zhang, S. Yan, P. Zhang, J. Ma, H.-Y. Chen, S. Huang, *Nat. Commun.* **2021**, *12*, 5811.
[37] S. Zhang, Z. Cao, P. Fan, W. Sun, Y. Xiao, P. Zhang, Y. Wang, S. Huang, *Angew. Chem., Int. Ed.* **2024**, *63*, 202316766.
[38] M. Faller, M. Niederweis, G. E. Schulz, *Science* **2004**, *303*, 1189.
[39] J. Cao, W. Jia, J. Zhang, X. Xu, S. Yan, Y. Wang, P. Zhang, H.-Y. Chen, S. Huang, *Nat. Commun.* **2019**, *10*, 5668.
[40] Y. Liu, T. Pan, K. Wang, Y. Wang, S. Yan, L. Wang, S. Zhang, X. Du, W. Jia, P. Zhang, H.-Y. Chen, S. Huang, *Angew. Chem., Int. Ed.* **2021**, *60*, 23863.
[41] Y. Liu, K. Wang, Y. Wang, L. Wang, S. Yan, X. Du, P. Zhang, H.-Y. Chen, S. Huang, *J. Am. Chem. Soc.* **2022**, *144*, 757.
[42] M. Pohanka, *BioMed Res. Int.* **2020**, *2020*, 3419034.
[43] N. G. Kowlgi, L. Chhabra, *Gastroenterol. Res. Prac.* **2015**, *2015*, 476215.
[44] J. P. Talasniemi, S. Pennanen, H. Savolainen, L. Niskanen, J. Liesivuori, *Clin. Biochem.* **2008**, *41*, 1099.
[45] Y. Liu, S. Zhang, Y. Wang, L. Wang, Z. Cao, W. Sun, P. Fan, P. Zhang, H.-Y. Chen, S. Huang, *J. Am. Chem. Soc.* **2022**, *144*, 13717.
[46] J. Uribarri, M. S. Oh, H. J. Carroll, *Medicine* **1998**, *77*, 73.
[47] Y. Chen, Q. Yao, L. Zhang, P. Zeng, *Front. Chem.* **2023**, *11*, 1289211.
[48] R. Ahmad, N. Tripathy, M.-S. Ahn, K. S. Bhat, T. Mahmoudi, Y. Wang, J.-Y. Yoo, D.-W. Kwon, H.-Y. Yang, Y.-B. Hahn, *Sci. Rep.* **2017**, *7*, 5715.
[49] G. Danaei, M. M. Finucane, Y. Lu, G. M. Singh, M. J. Cowan, C. J. Paciorek, J. K. Lin, F. Farzadfar, Y.-H. Khang, G. A. Stevens, M. Rao, M. K. Ali, L. M. Riley, C. A. Robinson, M. Ezzati, *Lancet* **2011**, *378*, 31.
[50] A. Diabetes, *Clin. Diabetes* **2021**, *39*, 14.
[51] S. Clement, S. S. Braithwaite, M. F. Magee, A. Ahmann, E. P. Smith, R. G. Schafer, I. B. Hirsch, *Diabetes Care* **2004**, *27*, 553.
[52] T. Scale, J. N. Harvey, *Clin. Endocrinol.* **2011**, *74*, 191.
[53] M. D. Levitt, D. G. Levitt, *Clin. Exp. Gastroenterol.* **2020**, *13*, 321.
[54] C. Zhang, X. H. Zhao, L. Yang, X. Y. Chen, R. S. Jiang, S. H. Jin, Z. Y. Geng, *Poultry Sci.* **2017**, *96*, 4325.
[55] A. R. Saltiel, C. R. Kahn, *Nature* **2001**, *414*, 799.
[56] J. Quick, N. J. Loman, S. Duraffour, J. T. Simpson, E. Severi, L. Cowley, J. A. Bore, R. Koundouno, G. Dudas, A. Mikhail, N. Ouédraogo, B. Afrough, A. Bah, J. H. J. Baum, B. Becker-Ziaja, J. P. Boettcher, M. Cabeza-Cabrerizo, Á. Camino-Sánchez, L. L. Carter, J. Doerrbecker, T. Enkirch, I. G. Dorival, N. Hetzelt, J. Hinzmann, T. Holm, L. E. Kafetzopoulou, M. Koropogui, A. Kosgey, E. Kuisma, C. H. Logue, et al., *Nature* **2016**, *530*, 228.
[57] Y. Wang, S. Yan, P. Zhang, Z. Zeng, D. Zhao, J. Wang, H. Chen, S. Huangs, *ACS Appl. Mater. Interfaces* **2018**, *10*, 7788.